

Transmission Line Model for Describing Power Performance of Electrochemical Capacitors

P.L. Moss and J.P. Zheng^{a*}

Department of Electrical and Computer Engineering, Florida A&M University and Florida State University, Tallahassee, FL 32310

^aalso Center for Advance Power Systems, Florida State University, Tallahassee, FL 32310

G. Au, P.J. Cygan, and E.J. Plichta

US Army CERDEC, Ft. Monmouth, NJ 07703

*Corresponding author: E-mail: zheng@eng.fsu.edu

Abstract

A simple equivalent circuit model for EC capacitors can be established based on electrochemical impedance spectroscopy. The circuit consists of an ohmic resistor and a finite-length Warburg Element in series. The EC capacitor's performance including the transient/pulse response and energy density as a function of power density (Ragone plot) can be simulated by the equivalent circuit model with three useful parameters including an ohmic resistance, total ionic resistance and total capacitance of the electrodes.

Key words: Electrochemical capacitors, Equivalent circuits, Warburg element

Introduction

Electrochemical (EC) capacitors are increasingly being used as electrical energy storage devices in a variety of applications due to their unique characteristics; these include, higher energy densities compared to conventional dielectric and electrolytic capacitors, and greater power densities and cycle life compared to rechargeable batteries.¹⁻⁶ Great efforts have been focused on increasing the energy density of EC capacitors including, optimization of the specific surface area and pore size of the activated carbon for increase double-layer capacitance;⁷⁻¹⁰ the development of pseudocapacitance electrode materials for increase energy storage per unit volume;¹¹⁻¹⁶ lately, the introduction of asymmetrical cell configuration.¹⁷⁻²¹ The theories on energy density of EC capacitors were also developed and successfully applied to double-layer capacitors and asymmetrical cells.²²⁻²⁶ The theoretical maximum energy density of EC capacitors and asymmetrical cells can be projected based on some basic parameters such as specific capacitance (or capacity) of the electrode, salt concentration in electrolyte, and operational voltage of the cell. The energy density theories can be used not only for predicting the maximum energy density of the capacitor but also to provide design parameters for achieving the maximum energy density. The parameters include the mass (volume) ratio between the electrode and electrolyte, porosity of the electrode for double-layer capacitor, and mass ratio between capacitive and battery electrode materials for asymmetrical cells. From the energy density theories, it was found that for most of current developed systems, the theoretical energy density was mostly limited by the salt concentration in the electrolyte.

The power density of the EC capacitor is determined by the internal resistances which include the electrical and ionic resistances. The detailed resistance distributions for EC capacitors with both bipolar and spiral-wound structures were investigated.^{27,28} The sources of electrical

resistance originates from the bulk resistance of the electrode material, contact resistance between activated carbon particles, current collector, and contact resistance between the carbon electrode and current collector. The sources of the ionic resistance are separator paper and ionic resistance in the porous electrode. The experimental results also demonstrated that the ionic resistance was a function of capacitor voltage, because the free ion concentration in the electrolyte decreased with the buildup of double-layer charges as capacitor voltage increase. However, even when the sources of internal resistance can be identified; the power density and the internal resistance of the double-layer capacitors cannot be related. The maximum peak power of the capacitor was sometime defined as the total energy divided by the internal resistance of the capacitor. It is also widely accepted that the best way to define the capacitor's performance is by using a Ragone plot,^{3,29,30} which describes the relationship between the energy density and power density. Currently, Ragone plot can only be obtained experimentally, and no model or theory exists to predict the relation between energy and power densities based on some basic parameters which can be easily obtained experimentally.

In this paper, we are going to demonstrated that an equivalent electrical circuit model can be established based on electrochemical impedance spectroscopy (EIS). The model consists of an ohmic resistance which represents all internal resistance within the capacitor except the ionic resistance from the porous electrode. It will be demonstrated that the total capacitance obtained from the equivalent circuit model is consistent with the capacitance values measured by dc charge-discharge method. It will also be demonstrated that the model can be use to describe the transient behavior of the capacitor, and for the first time to project the energy and power densities relationship.

Experimental

Electrochemical Impedance spectroscopy (EIS) measurements were carried out for a Panasonic electrochemical capacitor (2.5 V, 10 F: ØD =18 mm, L = 35 mm) using Solartron 1250B frequency response analyzer with windows PC control and data acquisition software by Zplot (Snibber Associates). All spectra were collected at open circuit voltage (OCV) using a 5 mV sinusoidal stimulus with frequency ranging from 10 mHz to 20 kHz in potential range of 0 to 2.5 V with spectra collected in increments of 0.5 V. The spectra are then fitted to an equivalent circuit using Zview software.

The dc charge-discharge was performed at constant current mode when the capacitor was charged and discharged between 0 and 2.50 V at ± 20 mA at ambient temperature. The capacitor under transient and pulsed response was measured under a pulse sequence of 1 A (2 sec.) to -0.5 A (2 sec.) to 0 A (1 sec.) to -0.5 A (2 sec.). The voltage profile was recorded by a Maccor battery test system. The capacitor was also discharged under constant power mode. The capacitor was first charged to 2.5 V and hold at the voltage until the current less than 5 mA; then the capacitor was discharged at different constant power from 0.045 to 10.7 W. The voltage profile during the discharge was also recorded by a Maccor battery test system. The maximum current capability of the system was 10 A.

Results and Discussion

Impedance spectroscopy measurements

EIS spectrum analysis in Fig. 1 shows that the frequency response of the EC capacitor is similar to that of the Warburg element in series with an inductive element and an ohmic

resistance. The inductive behavior (20 kHz – 632 Hz) is attributed to leads from the measurement setup and the spirally-wound structure of the capacitors, the ohmic resistance is observed at the Z' intercept of the real axis, and the Warburg element (632 Hz-10 mHz) with $\sim 45^\circ$ slop line represent the Warburg diffusion followed by a vertical line ($\sim 90^\circ$) that represents the accumulation of charge.

The impedance of the EC capacitor in the frequency domain can be represented by a series combination of inductor L, ohmic resistance R_o , and a Warburg impedance element Z_w shown in Fig. 2; in this model it is assumed that the Warburg element exhibits purely capacitive behavior at low frequencies. The response of the Warburg element in the frequency domain is given by the following formula:³¹

$$Z(j\omega) = \frac{\tau}{C_w} \frac{\coth(\sqrt{j\omega\tau})}{\sqrt{j\omega\tau}} \quad (1)$$

$\tau=R_wC_w$, and R_w and C_w are the sum of resistance and capacitance of the Warburg element shown in Fig. 2. For a porous electrode, R_w represents the effective resistance for ion transporting through the electrode, and C_w represents the total double-layer capacitance of the electrode. The experimental results measured at different bias voltages could be fitted well by an equivalent circuit model. From the fitting, three important parameters were obtained including the ohmic resistance $R_o=0.0655 \Omega$, the ionic resistance of the electrode $R_w=0.033 \Omega$, and the total capacitance of the electrodes, C_w , which was found to increase with increasing the bias voltage from 10.57 F at 0 V to 16.37 F at 2.5 V. These parameters will also be used to simulate the voltage profiles under pulsed current discharge and energy-power relationship of the capacitor. The inductance was also obtained and was about 0.757 μH ; however, it will not significantly affect the simulation results since the inductor value is small and its behavior only

be significant at high frequencies, e.g. above 632 Hz. Table 1 summarizes the resistance and capacitance obtained from the fitting of experimental EIS at different bias voltages.

DC Charge-discharge characterization

From the result of dc charge-discharge cycling, Fig 3, it can be seen that the V-t profile is triangular, with little variation in slope during charge-discharge; this indicates good capacitance characteristic with minimal variation in capacitance within this potential window. Based on the discharge portion of the V-t curve the capacitance was calculated using equation as expressed below:

$$C_{dl} = \frac{\Delta Q}{\Delta V} = \frac{i \times \Delta t}{\Delta V} \quad (2)$$

where i is the instantaneous discharge current, ΔV is the potential step and Δt is the differential discharge time. The internal resistance of the EC capacitor which is denoted by the equivalent series resistance (ESR) is determined from the transition between charge and discharge on the V-t curve and is given by:

$$R_{ESR} = \frac{\Delta V}{\Delta I} = \frac{\Delta V}{2I} \quad (3)$$

where ΔV is the change in voltage and I is the magnitude of charge and discharge current. The factor of 2 is because of that the current was switched from $+I$ to $-I$ at charge and discharge modes, respectively. The variation of capacitance with bias voltage was also obtained from the dc measurement and was listed in Table 1. It can be seen that within the bias voltage range 0-2.5 V the capacitance increased from a minimum of 14.62 F at 0V to a maximum of 16.64 F at 2.5 V. At the beginning of discharge (Fig. 3(b)) there is a sudden transition in potential between charge-

discharge. Using equation (3) an equivalent series resistance of 0.075 Ω was deduced from this transition.

To compare results obtained from EIS and dc charge-discharge, it can be seen that for both methods, values of capacitance and ohmic resistance can be obtained; however, the value of ionic resistance of the electrode can only be obtained from EIS method. The effects of R_w from the dc charge-discharge curve can be observed during the transition between charge and discharge on the V-t curve as shown in Fig. 3(b). The curvature after a sharp voltage drop was due to the ionic resistance of the electrode. A comparison of capacitance obtained by two different methods is shown in Fig. 4. It can be seen that the values of capacitance agree well at bias voltages higher than 1 V, however, the capacitance obtained from EIS is lower than that obtained from dc charge-discharge at bias voltages lower than 1 V. The possible explanation for the difference is that there is a very slow pseudocapacitance reaction occurred at one of the electrodes in the capacitor, because it was found that the total capacitance estimated based on the accumulated charge at low frequency increased with decreasing frequency, even at <10 mHz. The total capacitance was approximated by the following equation:

$$C_{dl} \approx \frac{1}{\omega Z''} \quad (4)$$

where ω is the frequency in rad/sec and Z'' is the imaginary component of the impedance in the complex plane.

Modeling system in time domains

A time domain representation of the equivalent circuit can be obtained by taking the inverse transformation of the impedance spectra in frequency domain. According to Mauracher,

the transformation or equivalent time domain representation (equation (4)) can be represented by:^{32,33}

$$\frac{k_1}{\sqrt{j\omega}} \coth\left(\frac{k_2}{k_1} \sqrt{j\omega}\right) \bullet - \circ \frac{k_1^2}{k_2} + \frac{2k_1^2}{k_2} \sum_{n=1}^{\infty} e^{-\frac{n^2 \pi^2 k_1^2}{k_2} t} \quad (5)$$

Comparing the parameters in equation (4) and left side of equation (5) resulting in

$$k_1 = \frac{\sqrt{\tau}}{C_w} = \sqrt{\frac{R_w}{C_w}} \quad (6)$$

and

$$k_2 = \frac{\tau}{C_w} = R_w \quad (7)$$

Then considering the impulse response for a parallel RC circuit given below by equation (8) and equation (5) it can be conclude that the Warburg element in the frequency domain have an equivalent time domain representation and can be express as a series combination of parallel resistive and capacitive elements.³⁴

$$\frac{1/C}{j\omega + 1/RC} \bullet - \circ \frac{1}{C} e^{-\frac{t}{RC}} \quad (8)$$

Also from equation (5), it is defined as:

$$C_o = \frac{k_2}{k_1^2} = C_w \quad (9)$$

Then, comparing equations (5) and (8) equate to the capacitance in each parallel branch given by equation (10)

$$C_n = \frac{k_2}{2k_1^2} = \frac{C_o}{2} \quad (10)$$

It can also be deduced from equations (5), (8), and (10) that

$$R_n = \frac{2\tau}{n^2\pi^2 C_o} = \frac{2R_w}{n^2\pi^2} \quad (11)$$

Finally, Fig. 5 shows the equivalent circuit of the EC capacitor in time the domain. The circuit includes a Warburg equivalent network, a series ohmic resistance R_o , and an inductive contribution L . Note that the leakage resistance is ignored in this model. The Warburg equivalent element represents diffusion into the porous electrode using a series/parallel RC network.

Transient response

Fig. 6 shows the voltage profile of EC capacitor in responded to a sequence of pulse currents of 1 A (2s) and -0.5 A (2s). The equivalent circuit model of Fig. 5 was applied using an experimental current input to stimulate the voltage profile. For the modeling using an equivalent circuit model as shown in Fig. 5, consider the condition when the EC capacitor is under constant-current load discharge, then the voltage around the loop result in a terminal load voltage given by:

$$v_L(t) = V_w - i_s R_o - L \frac{di_s}{dt} \quad (12)$$

where, i_s is the current through the capacitor, V_w is the voltage across the Warburg equivalent network and is given by

$$V_w = \sum_{n=0}^N V_n \quad (13)$$

The voltage on the capacitor C_o is the given by:

$$V_o = V_i - \frac{1}{C_o} \int_0^t i_s(t) dt \quad (14)$$

where, V_i is the initial voltage on the double-layer capacitor, C_o , The current in each parallel RC network is then given by:

$$i_c = i_s - i_p \quad (15)$$

and

$$i_p = \frac{V_n}{R_n} \quad (16)$$

where i_c and i_p are the currents in the parallel RC network respectively. The voltage on each parallel capacitor is then given by:

$$V_n = -\frac{2}{C_o} \int_0^t i_c(t) dt \quad (17)$$

The stimulated V-t profile was obtained using the Matlab/Simulink and also plot in Fig. 5 to compare with the experimental results. It is clearly seen the simulated terminal voltage show good agreement with the terminal voltage from the experimental. Buller et al³³ has successfully applied transmission line model to a practical load with much more dramatically current profile.

Power performance

Fig. 7 shows the V-t profiles of an EC capacitor discharged at constant power mode. Due to the maximum current limitation of the test system, the discharge process was stopped before

the capacitor reached the voltage of zero. The total time for discharge was obtained based on the fitting curve using a polynomial as shown in Fig. 7. The energy density as a function of power density (Ragone plot) can be obtained and is plotted in Fig. 8. Experimentally, at low power densities such as $< W/L$, the deliverable energy density is about 1.3 Wh/L; when power density is greater than W/L , the deliverable energy density drops rapidly.

To simulate the Ragone plot for a constant power (P) load connect to the EC capacitor, the active power drawn result in a terminal voltage given by:

$$v_L(t) = \frac{P}{i_s(t)} \quad (18)$$

The same set of equations (12)-(17) was used during the simulation, but the current i_s was not constant values and was determined by equation (18). The stimulated Ragone plot was also plotted in Fig. 8 in order to compare with the experimental results. During the stimulation, constant values of $R_o=0.0665 \Omega$ and $R_w=0.033 \Omega$ were used; however, a voltage dependent capacitance C_w was used. The capacitance values were determined by EIS measurement and linear fitting within two data points as shown in Table 1. It can be seen that at low power density, simulated result agrees well with the experimental result; however, at high power density, $>W/L$, the deliverable energy density was lower than the projected values by the equivalent circuit model. It is believed that the lower value obtained from the experimental power density is due ionic depletion in porous electrode. The total weight of electrolyte in EC capacitor was measured and is about 3.84 g. It is assumed that the salt concentration of electrolyte is 0.75 M/L. The total available charge from the electrolyte is about 234 C if it assumes 100% salvation. When the EC capacitor was fully charged to 2.5 V, the number of cations and anions, which are equivalent to charge of about 40 C would be accumulated at the double-layer of the negative and positive

electrodes, respectively. The change of such small number of ions should not affect the ionic resistance of the capacitor. It was also proven from the resistance measurements at different bias voltages. Both ohmic and ionic resistances in the electrode are almost constant in a voltage range of 0 and 2.5 V. However, it must be pointed out that when the capacitor was charged or discharged rapidly, the ion concentration and ionic resistance in the EC capacitor were not uniformly distributed, particularly in the electrode, which is dependent on the thickness of the electrode and pore size of activated carbon. Therefore, it is believed that at high power discharge and charge conditions, for these carbon surfaces with small pore size, the ion diffusion process was too slow that ion was either over saturated or depleted.

Effect of ionic resistance to power performance

The EC capacitor voltage behavior in response to a dynamic current profile is commonly modeled using the simple equivalent first order circuit shown in Fig. 9. This circuit consist three passive circuit elements that result in a first order approximation of the dynamic response of the EC capacitor. The circuit includes an equivalent series resistance, R_{ESR} , that represents the energy lost due to the distributive resistance of the electrolyte, electronic contacts and the porous separator; a double layer capacitance C_{dl} ; and an equivalent leakage resistance, R_p , that represents the long term capability of the capacitor to maintain charge. Fig. 10 shows the Ragone plots stimulated by a simple RC circuit model (R_p was ignored) and transmission line circuit model as shown in Fig. 5. For simplicity, a constant value of C_w was used. To compare Ragone plots obtained by the two different models, it can be seen that when $R_o \gg R_w$, the simple RC circuit model will be good enough to describe the energy and power relationship of the EC capacitor; however, when $R_o < R_w$, the RC circuit model cannot accurately project the maximum

power density of EC capacitors, which is limited by ionic resistance of R_w . From Fig. 10, it can also be seen that when R_o is reduced, the points at which the energy density starts to decline, increase with decreasing R_o , resulting in the increase in ultimate power density.

Fig. 11 shows that stimulated Ragone plots for the fixed R_o but variable R_w . It can be seen that when R_w increased, the energy density decreased; however, the ultimate power density was determined by the ohmic resistance (R_o) only. The relationship between the Ragone plots shown in Figs. 10 and 11 can be understood by the equivalent circuit shown in Fig. 2. The charges are stored in capacitors which formed the transmission line network. When charge is stored or released from the capacitors, they all must pass through the ohmic resistor R_o ; therefore, the value of R_o would determine the ultimate power density of EC capacitors. Charge stored or released from various capacitors in the transmission line network pass through different number of resistors in series as shown in Fig. 2. For the capacitors c_w that are closest to R_o , less resistance are available to block charge storage or release than those capacitors some distance away from R_o . The greater value of r_w means that the current decays faster along the capacitor distribution in the transmission line. Therefore, the ionic resistance influences the energy density of the EC capacitor.

Conclusion

An equivalent circuit model for EC capacitors was obtained from the impedance spectra and simulated in Matlab/Simulink. The result shows that accurate simulation of the terminal voltage under dynamic load current and constant power load can be achieved. The result also verifies the effectiveness of using CAD based tools in obtaining good estimates of the performance of EC capacitors under various load conditions. Additionally, the effect of ion

concentration change and depletion in porous electrode and separator paper can also be incorporated into the simulation. From Fig. 8, it is demonstrated an effective way to simulate at constant power over a range of energy densities the Ragone plot for an arbitrary EC capacitors. The advantages are cost, time, and optimization of cell design and performance.

This work was partially support by U.S. Army CERDEC.

References

1. E. Karden, S. Ploumen, B. Fricke, T. Miller, and K. Snyder, *Journal of Power Sources*, 168, 2 (2007).
2. J.N. Marie-Francoise, H. Gualous, R. Outbib and A. Berthon, *Journal of Power Sources*, 143, 275, (2005).
3. R. Kötz and M. Carlen, *Electrochimica Acta*, 45, 2483 (2000).
4. J.M. Miller, D. Nebrigic, and M. Everett, *Proceedings of The 16th International Seminar on Double Layer Capacitors*, Deerfield Beach, Florida, pp.22-33, December 4-6, 2006.
5. A. Burke, *Journal of Power Sources*, 91, 37 (2000).
6. J.P. Zheng, S.P. Ding, and T.R. Jow, "Ultracapacitor-Battery Hybrid Power Sources for Pulse Current Applications", *IEEE Transactions on Aerospace and Electronic Systems*, 37, 288 (2001).
7. D. Qu, *Journal of Power Sources*, 109, 403 (2002).
8. J. Chmiola, G. Yushin, Y. Gogotsi, C. Portet, P. Simon, P. L. Taberna, *Science*, 313, 1760 (2006).
9. R. K. Dash, A. Nikitin and Y. Gogotsi, *Microporous and Mesoporous Materials*, 72, 203, (2004).
10. H. Nakamura and M. Okamura, *Pocceedings of The 13th International Seminar on Double Layer Capacitors*, Florida Educational Seminars Inc. (2003).
11. J.P. Zheng and T.R. Jow, "A New Charge Storage Mechanism for Electrochemical Capacitors", *J. Electrochem. Soc.* 142, L6 (1995).
12. J.P. Zheng, "Ruthenium Oxide-Carbon Composite Electrodes for Electrochemical Capacitors", *Electrochem. and Solid-State Lett.* 2, 359 (1999).

13. S-L.Kuo, J-F. Lee, and N-L. Wu, *J. Electrochem. Soc.* 154, A34 (2007).
14. S-Y. Wang, K-C. Ho, S-L. Kuo, and N-L. Wu, *J. Electrochem. Soc.* 153, A75 (2006).
15. C. Lin, J.A. Ritter, and B.N. Popov, *J. Electrochem. Soc.* 146, 3155 (1999).
16. K.-C. Liu and M.A. Anderson, *J. Electrochem. Soc.* 143(1), 124-130 (1996).
17. G. G. Amatucci, F. Badway, A. DuPasquier, and T. Zheng, *J. Electrochem. Soc.* 148, A930 (2001).
18. S.M. Lipka, D. E. Reisner, J. Dai, and R. Cepulis, *Proceedings of The 11th International Seminar on Double Layer Capacitors*, Florida Educational Seminars Inc. (2001).
19. A. Laforgue, P. Simon, J. F. Fauvarque, J. F. Sarrau, and P. Lallier, *J. Electrochem. Soc.* 148, A1130 (2001).
20. T. Aida, I. Murayama, K. Yamada, and M. Morita, *Journal of Power Sources*, 166, 462 (2007).
21. S. Nohara, T. Asahina, H. Wada, N. Furukawa, H. Inoue, N. Sugoh, H. Iwasaki, and C. Iwakura, *Journal of Power Sources*, 157, 605 (2006).
22. J.P. Zheng, J. Huang, and T.R. Jow, "The Limitation of Energy Density for Electrochemical Capacitors", *J. Electrochem. Soc.*, 144, 2026 (1997).
23. J.P. Zheng and T.R. Jow, "The Effect of Salt Concentration in Electrolytes on The Maximum Energy Storage For Double Layer Capacitors", *J. Electrochem. Soc.*, 144, 2417 (1997).
24. J.P. Zheng, "The Limitation of Energy Density of Battery/Double-Layer Capacitor Hybrid Cells", *J. Electrochem. Soc.* 150, A484 (2003).
25. X. Wang and J.P. Zheng, "The Optimal Energy Density of Electrochemical Capacitor Using Asymmetrical Electrodes", *J. Electrochem. Soc.* 151, No.10, (2004).

26. J.P. Zheng, "The Theoretical Limitation of Energy Density for Electrochemical Capacitors with Intercalation Electrodes", *J. Electrochem. Soc.* 152, A1864 (2005).
27. J.P. Zheng, "Resistance Distributions in Electrochemical Capacitors with Bipolar Structure", *J. Power Sources*, 137, 158 (2004).
28. J.P. Zheng and Z.N. Jiang, "Resistance Distribution in Electrochemical Capacitors with Spiral-Wound Structure", *J. Power Sources*, 156, 748 (2006).
29. B. Pillay and J. Newman, *J. Electrochem. Soc.* 143, 1806 (1996).
30. Optimizing energy storage devices using Ragone plots, T. Christen and C. Ohler, *Journal of Power Sources*, 110, 107 (2002).
31. "Impedance Spectroscopy", ed. by J. P. Macdonald, John Wiley & Sons, New York, 1987.
32. P. Mauracher, "Modellbildung und Verbundoptimierung bei Elektrostraßenfahrzeugen," Ph.D. dissertation, RWTH Aachen, Germany, 1996.
33. S. Buller, E. Karden, D. Kok, and R.W. De Doncker, *IEEE Tran. Industry Applications*, Vol. 38, 1622 (2002).
34. J. David Irwin, "Basic Engineering Circuit Analysis", 8th ed. John Wiley & Sons, Inc., 2005.

Table 1 Summary of Resistance and Capacitance measured at different bias voltages

Bias Voltage (V)	0	0.5	1.0	1.5	2.0	2.5
R_o (Ω)	0.0655	0.0661	0.0642	0.0637	0.0642	0.0655
R_w (Ω)	0.0361	0.0282	0.0337	0.0332	0.0335	0.0355
C_w (F)	10.40	11.60	13.76	15.32	15.89	16.36
C_{dl} (F)	14.72	14.16	14.51	15.31	15.91	15.57

Figure Captions

Fig. 1 AC impedance spectra at different bias voltages.

Fig. 2 Electrochemical capacitor equivalent circuit model in the frequency domain.

Fig. 3 DC charge and discharge curves at constant current of 20 mA.

Fig. 4 The values of capacitance as function of bias voltage measured by ac impedance spectra and dc charge and discharge.

Fig. 5 Electrochemical capacitor equivalent circuit model in the time domain.

Fig. 6 Comparison of (a) simulation capacitor and experiment terminal voltage to response the pulsed current. The voltage difference between simulation and experimental is shown in (b), The current profile is shown in (c).

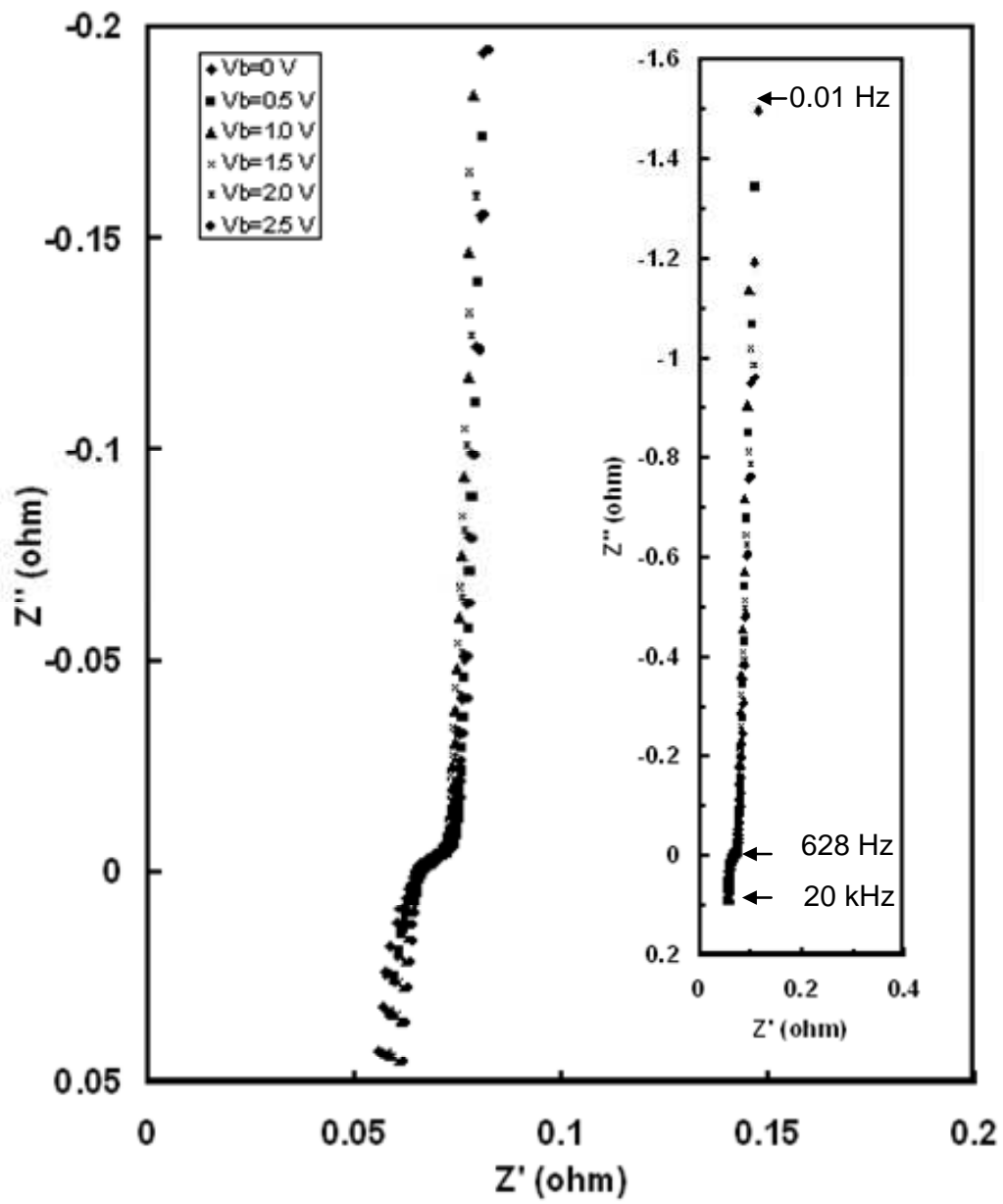
Fig. 7 The voltage profile for EC capacitor discharged at different powers. The line is a theoretical fitting using polynomial curves.

Fig. 8 Ragone plot of EC capacitor. The data points and the line obtain from experiment and stimulation using equivalent circuit model, respectively.

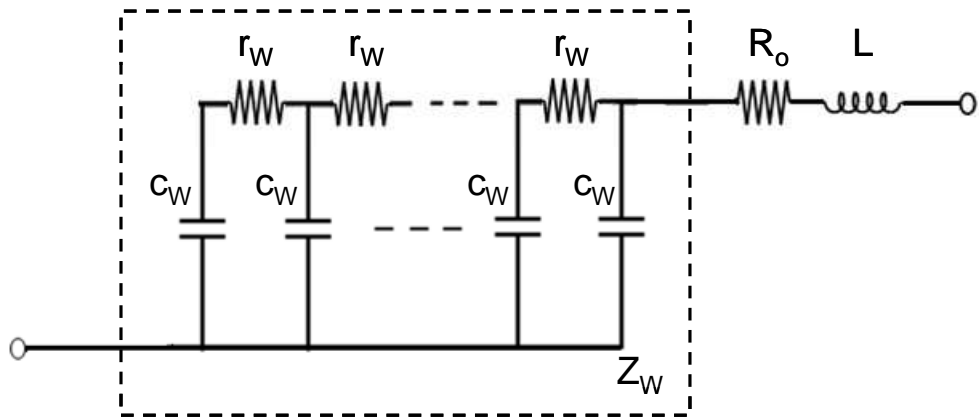
Fig. 9 The first order approximation for EC capacitor equivalent circuit.

Fig. 10 Stimulated Ragone plots using simple RC circuit (with small symbol) and transmission line circuit (with large symbol) models. For both models, the capacitance of 14 F was used and ohmic resistances were varied as indicated. The R_w for transmission line mode is 0.033Ω .

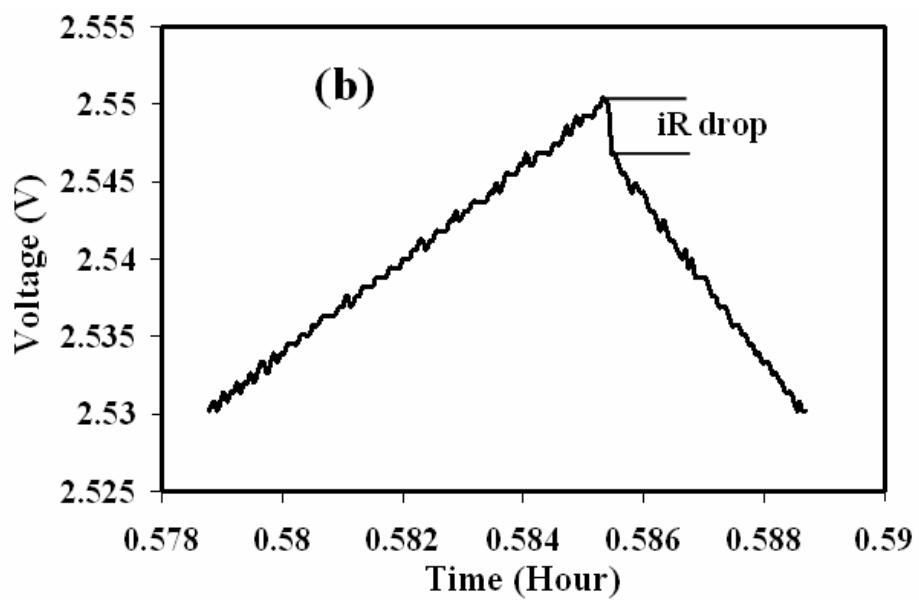
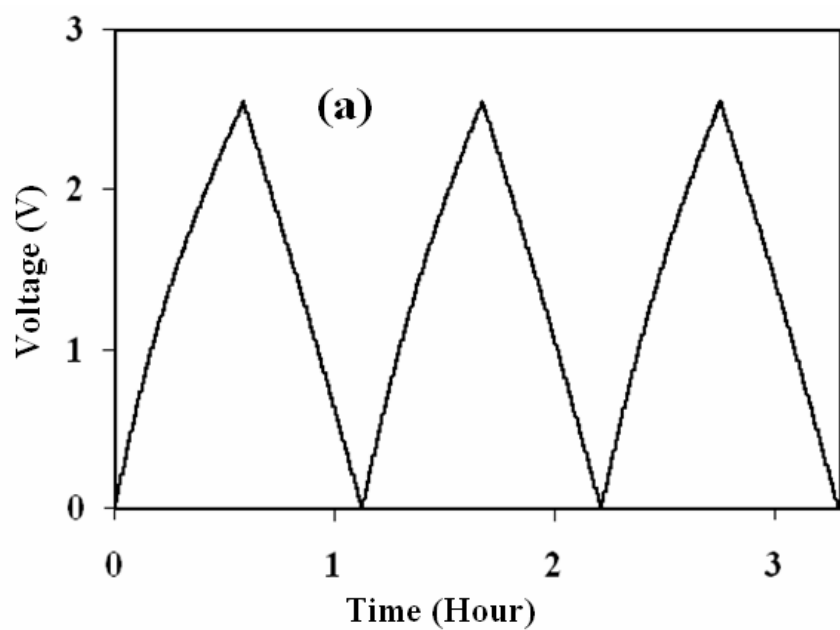
Fig. 11 Stimulated Ragone plots for various Warbury resistance R_w . The capacitance and ohmic resistance are 14 F and 0.066Ω , respectively.



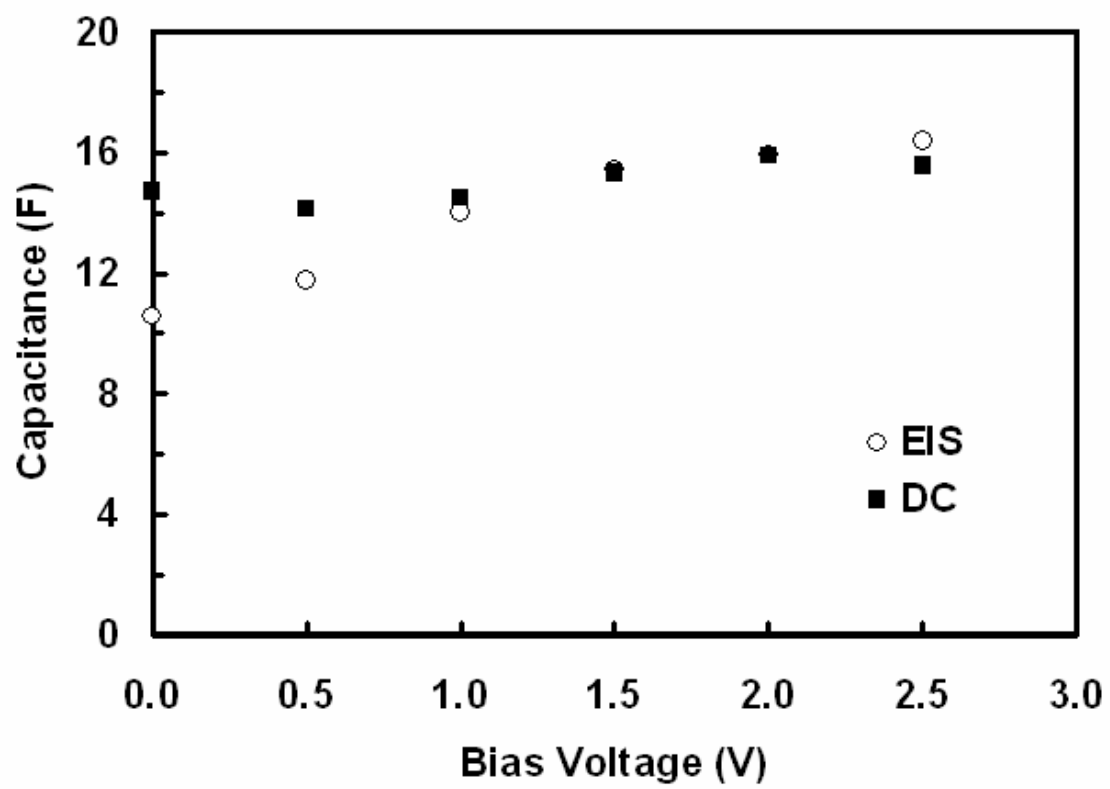
Moss et al. Fig. 1



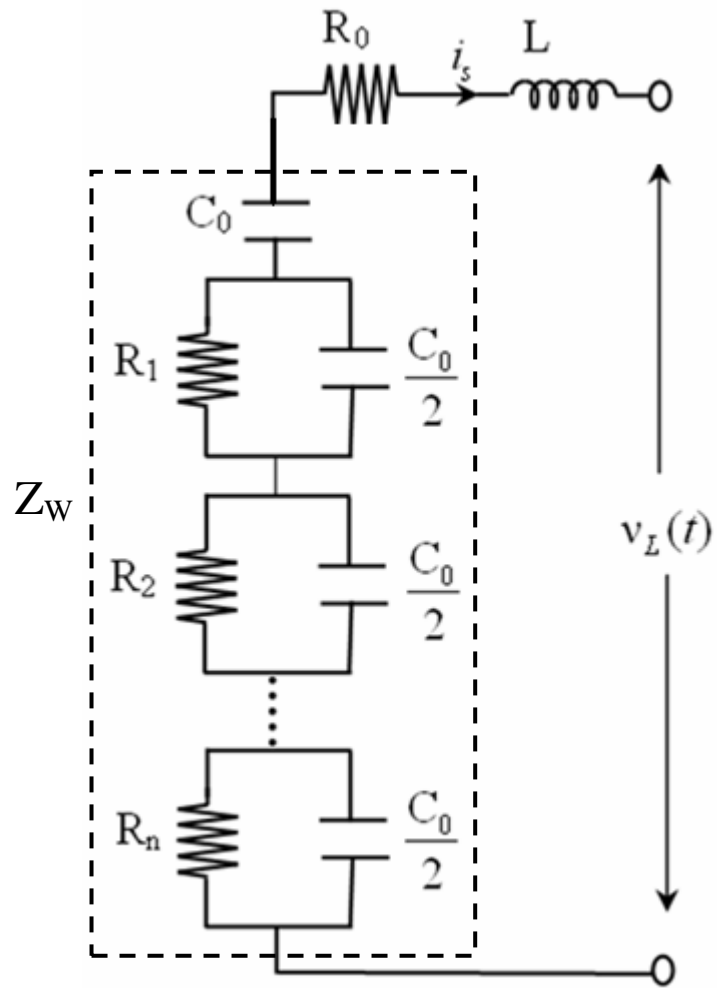
Moss et al., Fig. 2



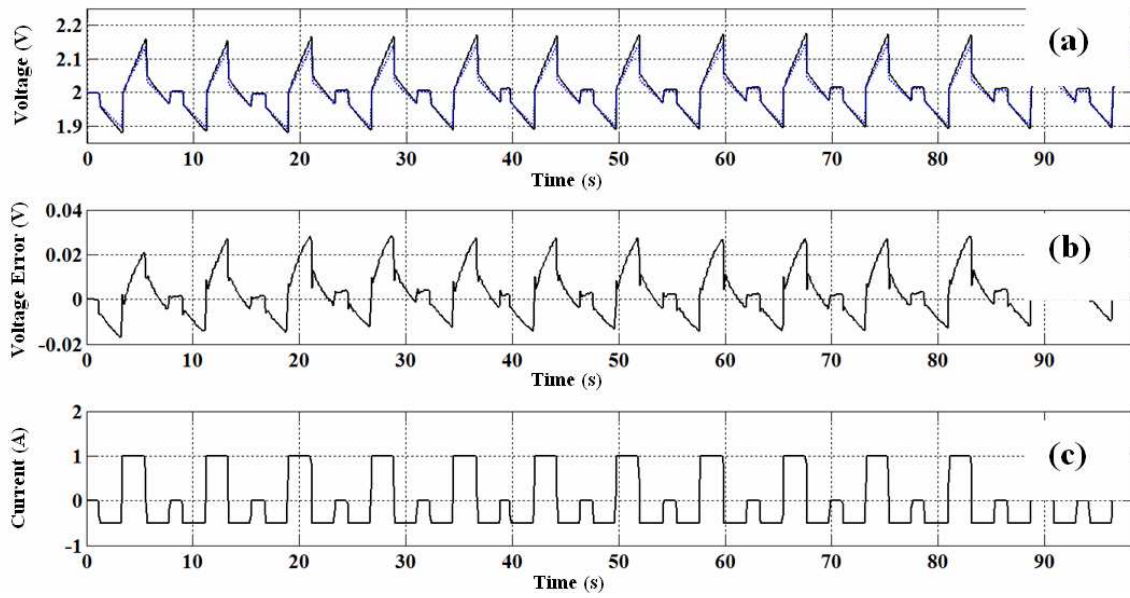
Moss et al., Fig. 3



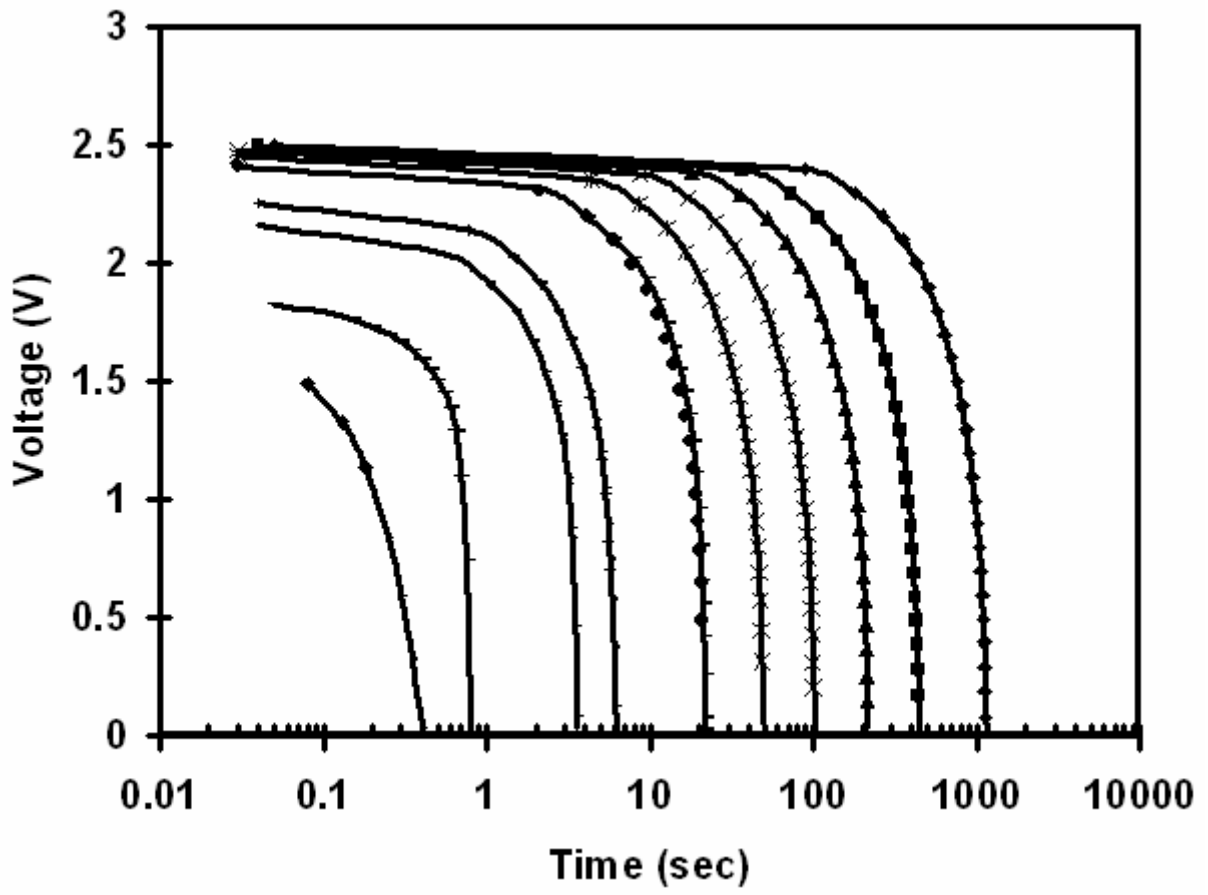
Moss et al., Fig. 4



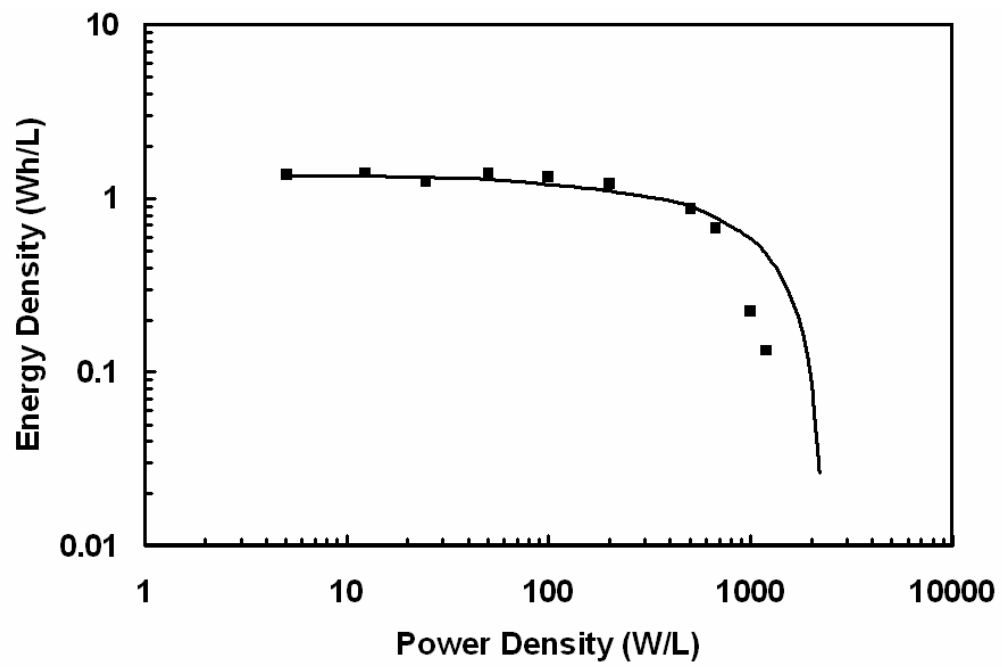
Moss et al., Fig. 5



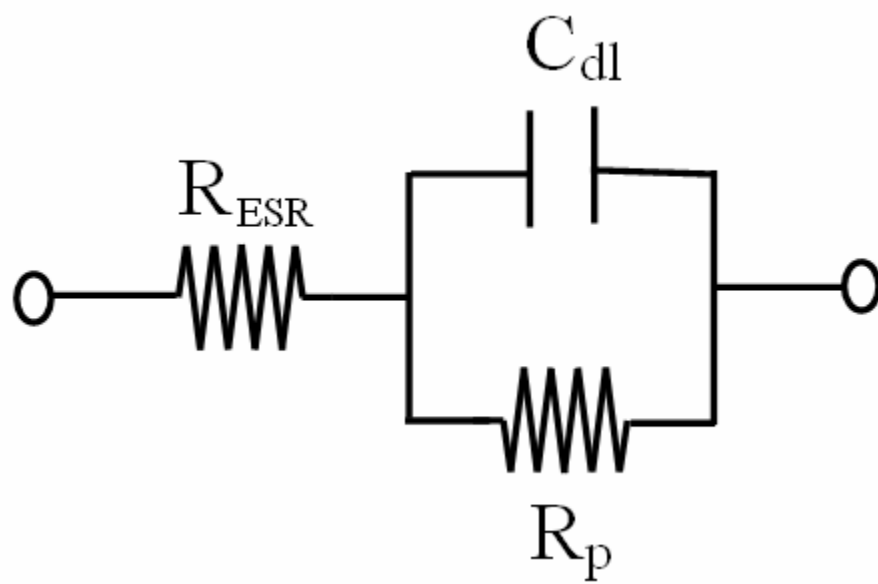
Moss et al., Fig. 6



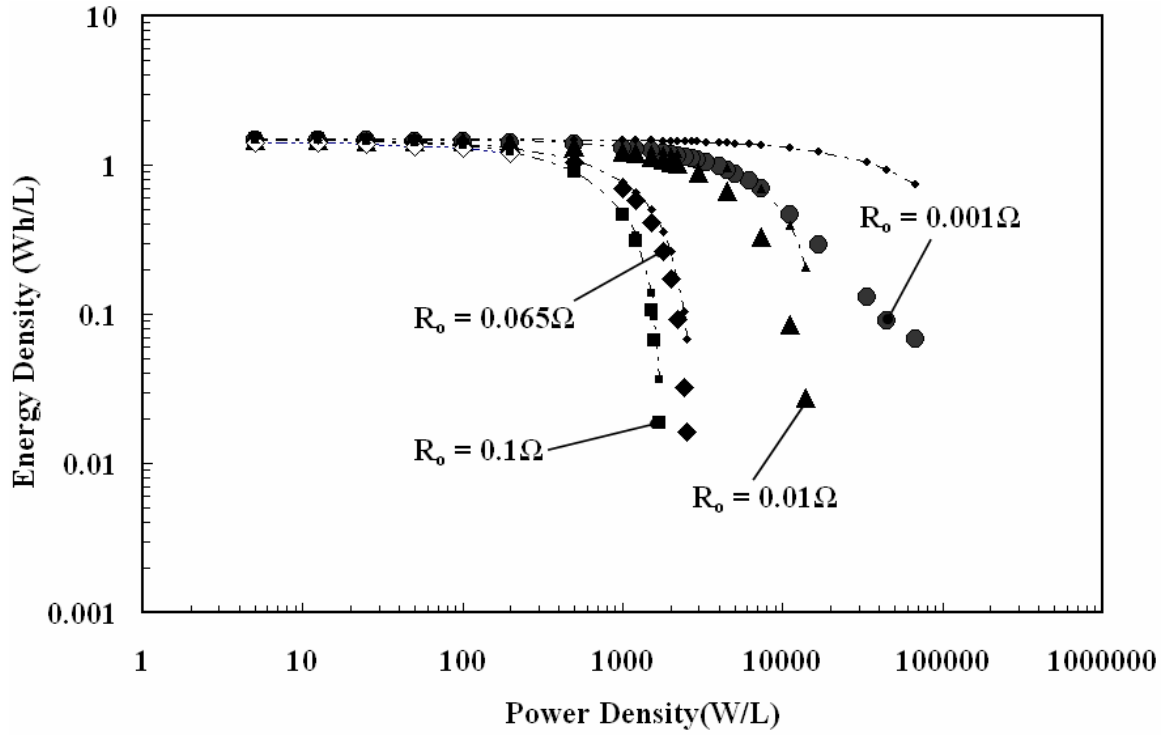
Moss et al., Fig. 7



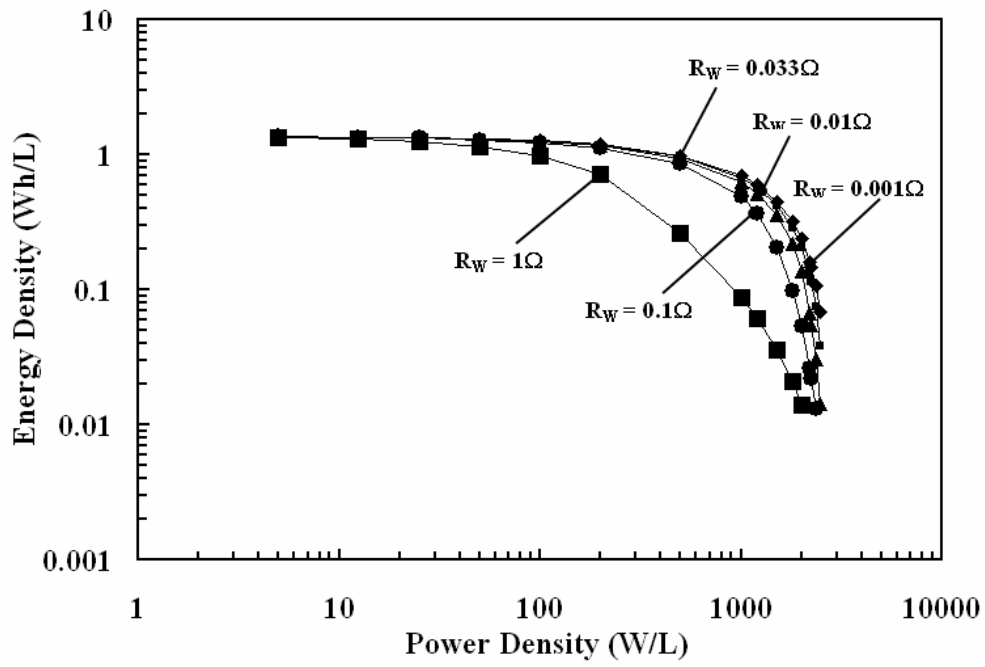
Moss et al., Fig. 8



Moss et al., Fig. 9



Moss et al., Fig. 10



Moss et al., Fig. 11